Available online at www.sciencedirect.com

Catalysis Today 99 (2005) 241–253

www.elsevier.com/locate/cattod

Reduction and re-oxidation of molybdena and vanadia: DFT cluster model studies

Renata Tokarz-Sobieraj, Małgorzata Witko*, Robert Gryboś

Institute of Catalysis and Surface Chemistry, PAS, ul. Niezapominajek 8, 30-239 Kraków, Poland

Abstract

Catalytic properties of oxide-based catalysts strongly depend on the mobility and reactivity of surface oxygen as well as on oxide ability to provide oxygen as a reactant and its facility to undergo re-oxidation process. To understand the whole process one of the most important information concerns energetics of creation and annihilation of surface oxygen vacancies. In order to obtain such data theoretical calculations by means of DFT method are carried out. Catalytic activity of different surface species that contain oxygen (surface O centers, surface OH and H_2O groups, adsorbed O_2) in MoO_3 and V_2O_5 systems are examined using cluster model. In addition, tendency towards an aggregation of surface oxygen vacancies is studied.

Keywords: Oxygen point defects; Molybdenum trioxide; Vanadium pentoxide; Surface oxygen centers; Re-oxidation; DFT cluster model study

1. Introduction

Transition metal oxides represent an important class of materials due to their technological and commercial importance [1–7]. In particular, two groups of catalytic materials, namely vanadium and molybdenum oxides – both pure and mixed with other metals, are well known catalysts for a whole spectrum of industrial processes. Vanadium- and molybdenum-based catalysts are active and selective in many chemical reactions of very different types. Vanadia-based compounds are used as components for catalysts used in mild oxidation, ammoxidation, oxidative dehydrogenation of hydrocarbons, selective oxidation of hydrocarbons, removal of NO_x, and selective reduction [8–13]. Molybdenum oxides in combination with other elements (bismuth, vanadium, cobalt, or aluminum) are applied as major catalysts in commercial processes such as isomerization, polymerization, production of formaldehyde, acronitrile and in particular, as selective catalysts for the partial oxidation of hydrocarbons and alcohols [14–18].

Catalytic properties of oxide-based catalysts depend strongly on the ability of oxide to provide surface oxygen as a reactant [1–21]. Therefore, it seems worthy to study chemical/catalytic properties of active oxygen centers as a function of both the coordination number (i.e. a number of chemical bonds that have to be broken) and the character of neighboring atoms (i.e. character of chemical bonds that have to be split off). On the other hand, the chemistry of transition metal oxides is strictly dependent on and controlled by the amount and properties of surface defects. Real crystal structure of transition metal oxides is characterized by presence of various ‘‘imperfections’’, described as defects of the crystal structure [22–28]. These defects are usually classified according to their dimensions and may be divided into point defects (vacancies; interstitial or foreign atoms), linear defects (dislocations), plane defects (shear planes, various internal/external grain boundaries) and spatial defects such as pores or foreign inclusions [2,8,14]. From a thermodynamic point of view an ideal crystal (with perfect periodical arrangement of all structural elements) can exist only at the temperature of absolute zero. At any other temperature thermal oscillations of surface atoms will lead to formation of various kinds of point defects decreasing the chemical potential.

---

* Corresponding author. Tel.: +48 12 425 2814; fax: +48 12 425 1923.
E-mail address: ncwitko@cyf-kr.edu.pl (M. Witko).

0920-5861/$ – see front matter © 2004 Elsevier B.V. All rights reserved.
doi:10.1016/j.cattod.2004.09.046

Some of the point defects (in particular oxygen vacancies) are formed during the catalytic reaction. In processes catalyzed by molybdenum or vanadium systems the Mars–van Krevelen [8,29] reaction mechanism gives two possibilities for the formation of oxygen point defects. First, through the formation and successive desorption of surface hydroxyl or water species, and second, via a direct incorporation of surface oxygen ions into an organic species. Surface hydroxyl and water species can be formed as a result of activation of hydrocarbon molecule on surface oxygen atoms, which are capable to abstract hydrogen atoms from the organic species, and can desorb in the subsequent step, leaving the oxygen point defects behind. The second reaction step, which is a nucleophilic oxygen insertion, proceeds through the transfer of surface oxygen atom(s) from the surface of oxide catalyst towards an adsorbed hydrocarbon and, as the result, gives the precursor of oxygenated product (aldehyde or ketone), which can desorb. Such an incorporation of surface oxygen atoms into the organic species creates also surface oxygen vacancy.

It is generally accepted that reduced surfaces often possess chemisorptive and catalytic properties different from stoichiometric surfaces [1–28] due to the different electronic configurations of the ions, and also different (lower in case of reduced surface) coordination of surface ions. Oxygen defect creates a new active site at the surface, which can be annihilated by either the diffusion of oxygen from the bulk or by an adsorption of atomic/molecular oxygen from a gas phase [3,28]. In a typical catalytic process the oxide surface undergoes step-wise reduction and oxidation. During the reduction the oxygen vacancies are formed and the parent structure is transformed first into a mixed-valence oxide and then into the lower-valence oxide (for example $V_2O_5 \rightarrow (V_4O_9, V_6O_{13}) \rightarrow VO_2 \rightarrow V_2O_3$ [8] or $MoO_3 \rightarrow (Mo_4O_{11}, Mo_{18}O_{52}) \rightarrow MoO_2$) [23]. At any step the reduction can be stopped and reversed by gaseous oxygen, which fills the vacancies and leads to re-oxidation of the surface. The combination of reduction/re-oxidation reactions together with structure transformation processes is a very complex phenomenon.

Formation or existence of surface oxygen vacancy might become a starting point for many different surface processes. Oxygen point defects may give rise to extended linear/planar defects, may initiate the creation of shear plane, and finally, may lead to a fully reduced oxide [23,30–34]. If the concentration of surface oxygen vacancies exceeds a critical value, the respective crystal plane changes its topology through rearrangements of the elementary metal–oxygen polyhedral units (for example from corner- into edge-linked), and in addition, the metal-to-oxygen ratio (stoichiometry) is modified. In effect, vacancies might become annihilated and different sub-oxide might be generated. The formation of crystallographic shear planes may be seen as one of the factors that create the ability of these structures to insert oxygen into the organic species in the selective oxidation process. However, one should stress that the formation of crystallographic shear planes cannot exclude the existence of point defects [35–39]. Experiments using ESR and EPR spectra postulate that the reduction of oxide surfaces proceeds at the beginning with the formation of structural point defects such as oxygen vacancy.

In recent years the electronic structure of point defects in metal oxide materials has received an increasing attention [23,24,40–50], due to a fact that understanding the nature of point defects in oxides is of a fundamental importance to catalysis. On one hand, the presence of reduced surface metal centers strongly affects the adsorption/activation of hydrocarbon molecules. In addition, surface point defects are responsible for the changes in optical, electronic and transport properties. On the other hand, the geometric and electronic nature of oxygen vacancies can change dramatically from system to system. On top of it one should remember that catalysts based on transition metal oxides usually exhibit pronounced crystallographic anisotropy, which causes the catalytic properties to be dependent on the exposed faces in a given crystalline sample. Further, the different oxide surfaces contain catalytic active sites, which usually participate in different elementary steps of catalytic reaction and, as the results, different types of oxygen vacancies exist at different surfaces.

Present paper aims at collecting and summing up the results of the ab initio DFT cluster studies, which consider two groups of catalytic materials, namely V–O and Mo–O systems. It focuses on the energetics of formation, aggregation and re-oxidation of oxygen point defects. To give complete, chronological picture of the changes occurring at any oxide surface (i.e. its reduction and re-oxidation) already published results, which concern formation of single oxygen vacancies [51–58] forego new material on creation of the second vacancy in presence of the first one, generation of the pair of vacancies and on aggregation of surface vacancies. For completeness the reverse of the surface reduction i.e. its re-oxidation done through the adsorption of O_2 gaseous molecule at different vacancies is considered [57,58]. The whole reduction/re-oxidation process that proceeds at surface of each oxide is discussed taking MoO_3 and V_2O_5 systems as examples. Changes in electronic structure connected with the vacancy formation are added.

2. Theoretical modeling

Vanadia- and molybdena-based catalysts have several common properties. First, both oxides contain metals exhibiting the highest oxidation states. Second, the crystal structures of both compounds consist of units where metal cations are surrounded by oxygen anions in octahedral coordination [59]. Those building units are connected with each other through edges and corners. The metal coordination sphere has not the highest possible symmetry because different M–O bond lengths distort it. Such a distortion results in the existence of structurally non-equivalent oxygen sites, especially at the surfaces and, in consequence, leads to the different types of oxygen vacancies having an impact on surface properties of both systems. To describe the non-equivalent oxygen sites/vacancies a finite cluster model is used. Geometry inside clusters follows from the crystallographic structure of the particular system. In all cases the selected clusters are representative for the discussed system, meaning that they contain all structurally different surface oxygen sites and elements that are characteristic for the surface geometry. The clusters are terminated by hydrogen atoms in order to saturate dangling bonds (resulting from the cutting of the cluster out of the surface) and to ensure proper formal oxidation states of metal and oxygen ions. Both oxides, MoO_3 and V_2O_5, crystallize in an orthorhombic layer type lattices, and may be viewed as systems of weakly bonded bi-layers (MoO_3) or single layers (V_2O_5) parallel to the (0 1 0) netplane.

In molybdenum trioxide each bi-layer consists of two interleaved planes of corner-linked distorted MoO_6 octahedra, where the octahedra of adjacent planes share edges. The (0 1 0) surface contains centers (see Fig. 1) of the following nature: O(1) terminal (molybdenyl) oxygen coordinated to one molybdenum atom through a short bond ($d_{\text{Mo–O}} = 1.67$ Å) that is almost perpendicular to the surface, O(2) bridging oxygen atom that lays asymmetrically between two Mo centers in the surface plane and bounds to them by short ($d_{\text{Mo–O}} = 1.73$ Å) and long ($d_{\text{Mo–O}} = 2.25$ Å) bonds, and finally O(3) bridging oxygen atom, placed symmetrically between two Mo centers of the surface layer ($d_{\text{Mo–O}} = 1.94$ Å) and linked to the third Mo center in the underlying sub-layer ($d_{\text{Mo–O}}$ = Mo–O distance 2.33 Å). The molybdenum center Mo(6) is coordinated to six oxygen atoms. To model the (0 1 0) surface the $Mo_{15}O_{56}H_{22}$ cluster is used (see Fig. 1).

Vanadium pentoxide, V_2O_5, is characterized by a layer-type orthorhombic lattice [59]. Loosely connected crystal layers, extending parallel to the (0 1 0) crystallographic plane, are described by a periodic arrangements of edge and corner sharing VO_5 square pyramids, pointing out at both sides of the layer. At the (0 1 0) surface the following surface centers, which are accessible for an incoming molecule, can exist (see Fig. 1): O(1) terminal (vanadyl) oxygen, coordinated to one vanadium atom through a short bond ($d_{\text{V–O}} = 1.58$ Å) perpendicular to the surface, O(2) bridging oxygen, laying in the surface plane and coordinated to two vanadium atoms by two equal bonds ($d_{\text{V–O}} = 1.78$ Å), and O(3) that bridges oxygen in the surface plane and is coordinated to three vanadium atoms, with two shorter V–O bonds ($d_{\text{V–O}} = 1.88$ Å) and one longer bond ($d_{\text{V–O}} = 2.02$ Å). In addition, there exist V(5) bare vanadium centers coordinated to five oxygen atoms. In the calculations the local environment at the (0 1 0) surface is modeled by $V_{10}O_{31}H_{12}$ cluster (see Fig. 1), which describes different surface oxygen centers.

Point defects created at the surface are described using $Mo_{15}O_{55}H_{22}$ and $V_{10}O_{30}H_{12}$ clusters that are obtained by removing oxygen from structurally different positions at the respective surface. Each local defect obtained in that way results from different number of broken bonds and has a different chemical/geometrical arrangement.

The calculations are carried out by means of ab initio DFT method [60,61], using StoBe quantum chemistry program package [62]. The exchange correlation interactions are accounted for by the gradient corrected RPBE functional [63,64]. The Kohn–Sham molecular orbitals are expanded as a linear combination of atom-centered Gaussian-type orbitals, expressed in terms of double zeta basis sets including polarization functions. For vanadium, oxygen, and hydrogen atoms extended all electron basis sets are used, whereas molybdenum atoms are represented by valence basis sets with the $[Ar]3d^{10}$ core described by a

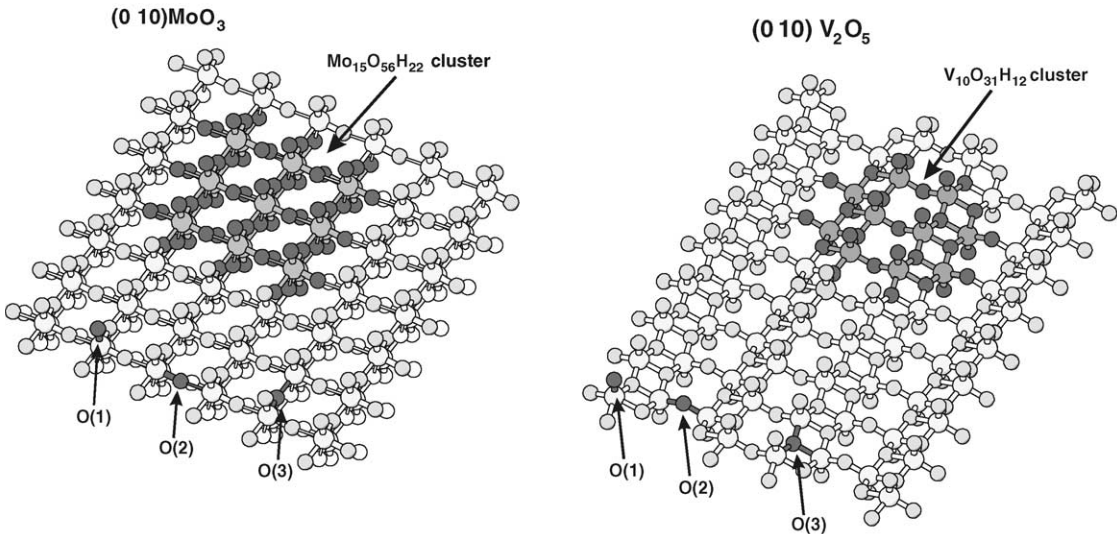

Fig. 1. Sketch of non-equivalent oxygen centers (black dots), O(1–3), at the (0 1 0)MoO_3 and (0 1 0)V_2O_5 surfaces. Additionally the substrate clusters $M_{15}O_{56}H_{22}$ and $V_{10}O_{31}H_{12}$ used to represent (0 1 0)MoO_3 and (0 1 0)V_2O_5 surfaces respectively are emphasized.

model core potential [65]. The details of the electronic structure of the studied systems are explored using the Mulliken analysis [66], Mayer bond order indices [67,68], and atom projected densities of the states (PDOS). In addition, the changes in cluster geometry as consequences of bond making/breaking are discussed. To describe the problem of trapping electrons at the surface vacancy two different strategies are applied. Starting from the hypothesis that the removal of an oxygen atom leads to the formation of dangling bonds [69,70] no basis function is placed at the position of missing oxygen. In the second approach assuming the possibility of electron localization (observed in ionic systems, like MgO [71,72]) the basis set of the missing oxygen is put into the vacancy place.

3. Results and discussion

3.1. Energetics of point defects at perfect surfaces

The thermodynamic stability of various oxygen sites at the surfaces is directly connected with the energy required to remove an oxygen species from the surface. Generally, at both studied surfaces, three different types of surface oxygen vacancies can exist: O(1) vacancy created by removing singly coordinated terminal oxygen atom, O(2) vacancy formed after desorption of doubly coordinated oxygen, and O(3) vacancy localized in the place of triply coordinated oxygen. Fig. 2 shows all types of studied oxygen vacancies in Mo–O and V–O systems.

Depending on the electronic charge of the removed oxygen species (neutral O atom or charged O^- and O^{2-} oxygen ions), surface vacancies can exist in three electronic states: 0, −1 or −2 – when O^{2-}, O^- or O is removed, what corresponds to the 2+, 1+ and 0 charged clusters, respectively. Generally, the process of vacancy formation can be represented by the following formal reaction:

$$\text{ideal surface} \rightarrow (\text{surface with point defect})^{n+} + (\text{oxygen species})^{n-}, \quad n = 0, 1, 2$$

Based upon the clusters model, the energy of vacancy formation, that is equal to the energy needed to desorb surface oxygen species, $E_D(O)^n$, is defined by an equation following from the total energies of the appropriate clusters and oxygen species:

$$E_D(O)^n = E_{tot}(M_xO_{y-1}H_z)^{n+} + E_{tot}(O)^{n-} - E_{tot}(M_xO_yH_z)$$

where $E_{tot}(O)^{n-}$ and $E_{tot}(M_xO_yH_z)$ are ground state total energies of the free oxygen species and the non-defected cluster (without vacancy) and $E_{tot}(M_xO_{y-1}H_z)^{n+}$ is the total energy of the defected (with an oxygen vacancy) cluster.

Preliminary studies on the removal of oxygen ions (O^- and O^{2-}), resulting in the charged vacancies, which are done for Mo–O and V–O–P systems, show that at oxide surfaces neutral vacancies form more stable local defects than

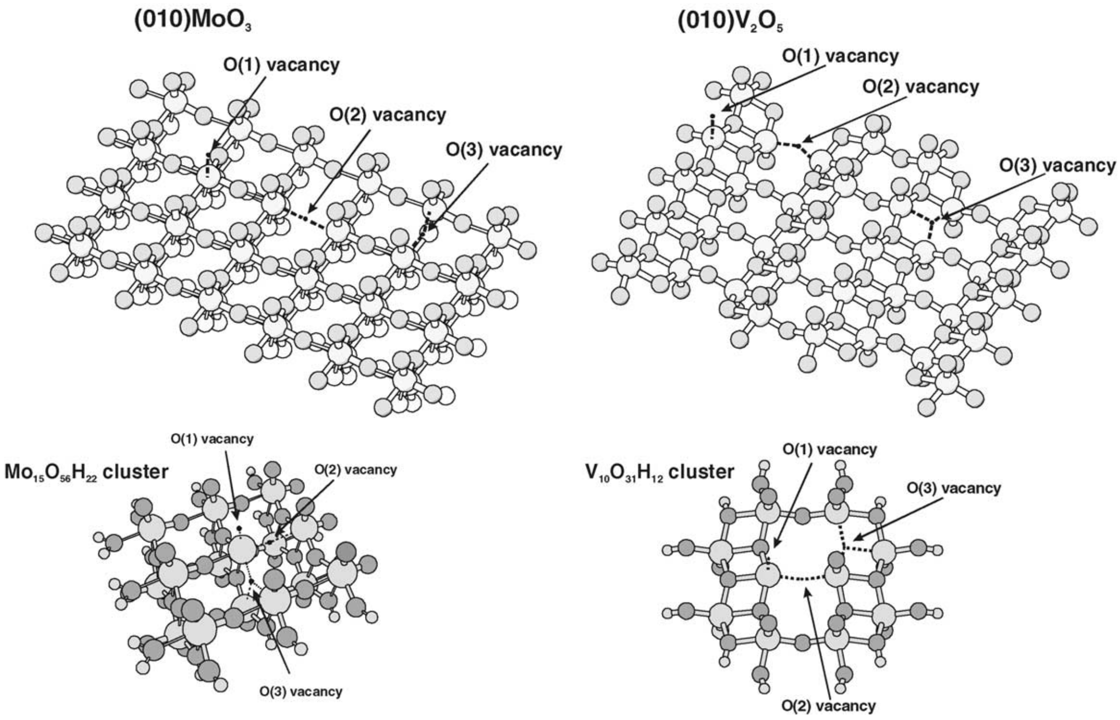

Fig. 2. Sketch of the vacancies at different surface oxygen sites O(1–3) at the (0 1 0)MoO_3 and (0 1 0)V_2O_5 surfaces and additionally in the $M_{15}O_{56}H_{22}$ and $V_{10}O_{31}H_{12}$ clusters used to represent studied surfaces. Arrows indicate positions of created point defects at various sites at surfaces and in the cluster.

charged vacancies. The energy needed to create any positively charged vacancy is much higher than energy required to obtain neutral vacancy. This does not mean that charged vacancy cannot act in the catalytic process, however, taking into account that catalyst forms the electron reservoir, one should expect the neutralization of any local defect. To keep this in mind only neutral oxygen vacancies are taken into account in the following discussion and for clarity the superscript "*n*" is from now on omitted.

Table 1 lists energies needed to form surface vacancies. All values are obtained keeping atoms in their bulk positions. For each system the first row of the table defines energy required to remove surface oxygen atom from non-defected surface. High, positive values of the defect formation energies indicate that creation of oxygen vacancies at transition metal surfaces is a strongly endoenergetic processes.

The results of calculations show that the energy of vacancy formation is a function of defect location, i.e. depends on the coordination of removed oxygen atom, which is connected with the number of bonds that have to be broken. All oxygen atoms are very strongly bound to their substrate environment and are unlikely to be removed in one step during the catalytic reaction. The vacancy energies, E_D, vary between 6.50 and 6.80 eV for MoO_3 and from 6.55 to 7.47 eV for V_2O_5. In the MoO_3 system, the energy of vacancy formation is slightly larger for singly and doubly coordinated oxygen atoms, O(1) and O(2), than for triply coordinated O(3). For V_2O_5, the energy of vacancy formation is largest for two-fold bridging site O(2) while those connected with O(3) and O(1) sites are smaller by 0.92 and 0.86 eV, respectively. In both oxides energies needed to remove oxygen atoms with the same coordination number but bound to different metal ions (Mo, V), are similar, except doubly coordinated oxygen atom, O(2). The energy needed to remove this type of oxygen is larger for V_2O_5 (E_D = 7.47 eV) than for MoO_3 (E_D = 6.75 eV). It is probably due to the coordination type of O(2) site in MoO_3 system, where the doubly coordinated bridging oxygen is bounded to the Mo center by one short (strong) and one long (weak) bonds and, as the result, it posses many properties of the singly bonded oxygen O(1), having an impact on the vacancy creation energy that is similar to O(1) site.

Table 1
Defect formation energies [eV] for the surface oxygen sites O(1–3) coordinated to one, two and three metal ions, respectively at perfect and defected surfaces for MoO_3 and V_2O_5

MoO_3	Energy of vacancy formation [eV]	V_2O_5	Energy of vacancy formation [eV]
O(1)	6.80	O(1)	6.61
O(2)	6.75	O(2)	7.47
O(3)	6.50	O(3)	6.55
Energy of O(1) vacancy formation in presence of			
O(1)	6.64	O(1)	6.52
O(2)	6.37	O(2)	7.05
O(3)	6.38	O(3)	6.76
Energy of O(2) vacancy formation in presence of			
O(1)	6.32	O(1)	7.91
O(2)	6.62	O(2)	7.50
O(3)	6.40	O(3)	7.64
Energy of O(3) vacancy formation in presence of			
O(1)	6.08	O(1)	6.71
O(2)	6.15	O(2)	6.72
O(3)	6.54	O(3)	6.88

All values obtained with the cluster model (details in the text), using a DFT non-local (RPBE) functional.

3.2. *Energetics of point defect formed at defected surface*

The energy of vacancy formation is different, when the vacancy is created at already defected surface i.e. at surface with local oxygen vacancy. To study the influences of existing point defects on the energy needed to create a new vacancy in already defected material, a two-step process of di-vacancy formation is studied. The energy required to create a surface vacancy next the pre-existing single vacancy is defined by the formula:

$$E'_D(O) = E_{tot}(M_xO_{y-2}H_z) + E_{tot}(O) - E_{tot}(M_xO_{y-1}H_z)$$

where $E_{tot}(M_xO_{y-2}H_z)$ is the total energy of the cluster with two types of oxygen vacancies, $E_{tot}(M_xO_{y-1}H_z)$ is the total energy of the cluster with mono-vacancy and $E_{tot}(O)$ is the ground state of the free oxygen species. In all cases removing two closest oxygen atoms forms two vacancies. This value should be discussed with respect to the results concerning isolated vacancies. Table 1 summarizes the energy values for MoO_3 and V_2O_5 systems. For each system we have three groups that list energies needed to form different types of mono-vacancies (discussed before). Consecutive rows contain energies required to create a particular type of vacancy *in the presence* of another, already present vacancy (as indicated by the labels).

Analysis of the results indicates the existence of a strong interaction between oxygen vacancies at surfaces. In the case of MoO_3, for almost all vacancy dimers (except the O(3)–O(3) vacancy pair) the formation energy of the second vacancy is smaller than the respective value for non-defected system. For example: the formation of O(2) type vacancy in a "perfect" crystal costs 6.75 eV, whereas, when O(1) type or O(2) type vacancy exists at the surface, creation of the same type of oxygen vacancy cost 0.43 or 0.35 eV less. Similar effect exists for other vacancies. Formation of O(1) vacancy is easier in the presence O(2) or O(3) vacancy (energies lower by 0.43 or 0.42 eV, respectively) whereas creation of O(3) is energetically less costly (by 0.42 or 0.35 eV) in the presence of O(1) or O(2) type vacancy. In MoO_3 system the pre-existing vacancies, which are of the different type than the vacancy being created, lower the required energy more than the vacancy of same type with respect to the one being formed. Energy needed to create the second homo (with respect to the first) vacancy is lower by 0.16 and 0.13 eV for O(1) and O(2) type, respectively.

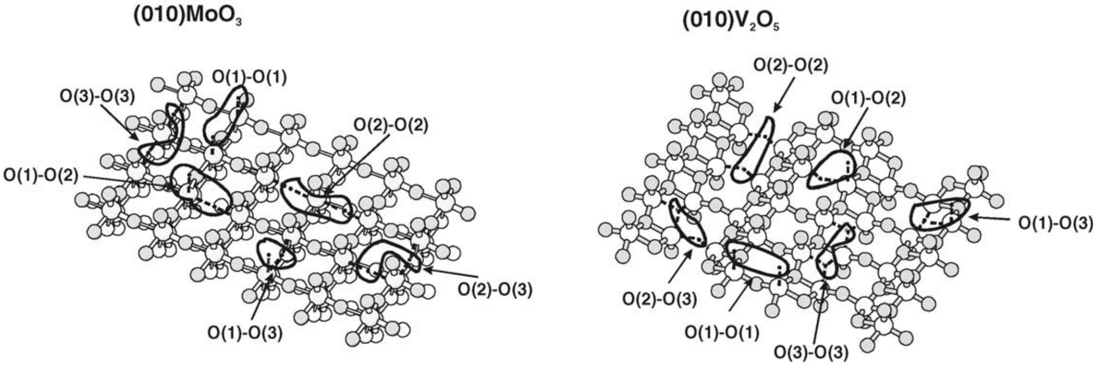

Fig. 3. Models for different di-vacancy complex at (0 1 0)MoO_3 and (0 1 0)V_2O_5 surface.

Formation of the second O(3) type vacancy (at surface where already O(3) vacancy exists) costs a bit more than the formation of first O(3) vacancy.

In contrast to MoO_3, in the V_2O_5 system, independently of the sequence of vacancy formation, the energy needed to generate the second vacancy site is always larger then respective energy associated with formation of a point defect on the ''perfect'' surface. For example: the formation of O(2) type vacancy in the presence of O(1) or O(3) vacancy costs 0.44 or 0.17 eV more than the creation of the first O(2) type vacancy. The same is true for O(3) vacancy formed when already O(1) or O(2) vacancy exists at the surface (the needed energies are larger by 0.16 or 0.17 eV, respectively) and for O(1) vacancy created in the presence of O(2) or O(3) (energies larger by 0.44 or 0.15 eV). Only in the case of O(1)–O(1) dimer, formation of O(1) type vacancy nearby O(1) vacancy is favorable and costs less (6.52 eV) than the creation of O(1) type vacancy on a ''perfect'' surface (energy equals to 6.61 eV).

3.3. Energetics of di-vacancies

The electrostatic interaction between point defects may lead to the association and formation of pairs (dimers) of vacancies and further to larger aggregates such as line, plane and spatial defects. Therefore selected models with different di-vacancy complexes on nearest-neighboring oxygen sites, for MoO_3 and V_2O_5 systems are considered (see Fig. 3).

Studies on all di-vacancy configurations obtained in one-step process serve as a test for the tendency of vacancy aggregation at the surface. The energy required to form pair of vacancies, E_D(O–O), is defined in a way analogous to isolated vacancies i.e. by subtracting total energy of the perfect cluster, $E_{tot}(M_xO_yH_z)$, from the sum of the total energies of cluster with di-vacancy, $E_{tot}(M_xO_{y-2}H_z)$, and two extracted oxygen atoms, $E_{tot}(O)$:

$$E_D(O{-}O) = E_{tot}(M_xO_{y-2}H_z) + 2E_{tot}(O) - E_{tot}(M_xO_yH_z)$$

Table 2 summarizes the corresponding energies of oxygen di-vacancy formation as a function of defect location (first row for each system), together with energies of accumulation, E_{acc}, defined as a difference between the energy required to form a di-vacancy, E_D(O–O), and the sum of energies associated with formation of two isolated vacancies of the given types, E_D(O):

$$E_{acc} = E_D(O{-}O) - 2E_D(O)$$

The negative value of energy E_{acc}, implies the gain in energy of aggregated di-vacancy with respect to two isolated vacancies.

Negative values of accumulation energy, E_{acc}, in the MoO_3 oxide suggest that the process of di-vacancy formation is more favorable than the existence two isolated vacancies at the surface. The energy gain is the largest (equal to −1.10 eV) for O(2)–O(2) dimer where single Mo atom looses two neighbors and changes its coordination from 6 to 4. Note that a similar decrease in Mo coordination number caused by O(3)–O(3) vacancy accumulation is much less favorable (E_{acc} = −0.23 eV). In general, the hetero-type dimers, O(1)–O(2), O(1)–O(3), O(2)–O(3) exhibits lower

Table 2
Di-vacancy formation energy [eV] E_D(O–O) and energy of accumulation of oxygen vacancies E_{acc} [eV]

	Energy of di-vacancy formation [eV]					
	O(1)–O(1)	O(1)–O(2)	O(1)–O(3)	O(2)–O(2)	O(2)–O(3)	O(3)–O(3)
MoO_3						
E_D(O–O)	13.50	13.12	12.88	13.68	12.90	12.77
E_{acc}	−0.16	−0.43	−0.41	−1.10	−0.34	−0.23
V_2O_5						
E_D(O–O)	13.13	14.52	13.32	14.81	14.19	13.13
E_{acc}	−0.08	0.45	0.16	0.03	0.17	0.02

E_{acc} (between −0.34 and −0.43 eV) than homo-type dimers that are formed by the same type of oxygen vacancies i.e. O(1)–O(1), O(3)–O(3) (−0.16 and −0.23 eV). This means that in MoO_3, independently of what type of mono-vacancy is created in the first step, formation of another vacancy nearby is favorable in comparison with the creation of two isolated vacancies.

In the case of V_2O_5, in contrast to MoO_3, the association energy is positive (or at least only slightly negative) for all cases. Homo-type dimers seem not to interact with each other since all accumulation energies are close to zero; E_{acc} equals to −0.08, 0.02 and 0.03 eV for O(1)–O(1), O(2)–O(2), and O(3)–O(3) dimers, respectively. For hetero-type dimers, positive values of accumulation energy varying from 0.16 to 0.45 eV, indicate mutual repulsion, and as a result, the second vacancy is expected to reside as far away from the first one as possible. In almost all cases the energy required to extract the second atom in order to form a di-vacancy at (0 1 0)V_2O_5 surface, is higher than that required to create the respective additional mono-vacancy at infinite distance. Therefore, the di-vacancy complex should be rather unstable.

3.4. Formation of oxygen point defects in the presence of H

It is generally accepted that oxygen vacancies are formed easily in reducing atmosphere, i.e. in hydrogen presence. Hydrogen, which is always present near the surface, may adsorb at oxygen site to form surface hydroxyl (OH group) that may subsequently desorb leaving the vacancy behind. Similarly, the hydroxyl group may interact with another hydrogen atom to form surface water species, which may desorb in the next step, resulting in the formation of oxygen vacancy at the surface. Therefore different scenarios of vacancy formation are possible:

$$(O)_{surf} \rightarrow (O)_{des},$$
$$(O)_{surf} + H \rightarrow (OH)_{surf} \rightarrow (OH)_{des},$$
$$(OH)_{surf} + H \rightarrow (H_2O)_{surf} \rightarrow (H_2O)_{des}$$

which means that the oxygen vacancies at transition metal oxides can be created in three different ways: by direct removal of surface O atoms from structurally different positions at the surface (energetics of this process were discussed above), by adsorption of H atoms at the surface O atoms followed by formation OH groups and desorption of hydroxyl groups, or through adsorption of another H atom at surface OH group, formation of surface water species and its desorption.

Table 3 collects the energy data corresponding to creation of vacancy via removal of surface oxygen atom and through abstraction of OH and H_2O surface species, for MoO_3 and V_2O_5 systems. Some of the results have been already published [52–54] but are repeated for completeness. The energies required to create a vacancy at the surface by abstracting different surface species are defined by the following formulas:

Table 3
Energy of vacancy formation by removal of oxygen atom, OH and H_2O group from the (0 1 0)V_2O_5 and (0 1 0)MoO_3 surface

	E_D(O) [eV]	E_D(OH) [eV]	E_D(H_2O) [eV]
MoO_3			
O(1)	6.80	4.51	1.47
O(2)	6.75	4.11	−0.20
O(3)	6.50	3.12	–
V_2O_5			
O(1)	6.61	4.67	1.17
O(2)	7.47	5.33	0.92
O(3)	6.55	4.06	0.08

$$E_D(O) = E_{tot}(M_xO_{y-1}H_z) + E_{tot}(O) - E_{tot}(M_xO_yH_z),$$
$$E_D(OH) = E_{tot}(M_xO_{y-1}H_z) + E_{tot}(OH) - E_{tot}(M_xO_yH_z)H,$$
$$E_D(H_2O) = E_{tot}(M_xO_{y-1}H_z) + E_{tot}(H_2O) - E_{tot}(M_xO_yH_z)2H$$

where $E_{tot}(M_xO_{y-1}H_z)$ is the energy of the cluster with oxygen vacancies; $E_{tot}(M_xO_yH_z)$, $E_{tot}(M_xO_yH_z)H$, and $E_{tot}(M_xO_yH_z)2H$ are the total energies of the ‘‘perfect’’ cluster, cluster with hydrogen adsorbed, and cluster with two hydrogen adsorbed, whereas $E_{tot}(O)$, $E_{tot}(OH)$, $E_{tot}(H_2O)$ are ground state energies of the free O, OH and H_2O species, respectively.

Results of calculations clearly show, that presence of hydrogen facilitates formation of oxygen vacancies. The energies of hydroxyl or water removal from the surface are always smaller than corresponding values for the removal of individual surface oxygen. The energies needed to form vacancy through desorption of OH species are reduced by at least 40–50% in comparison to surface oxygen desorption. The energy of OH desorption ranges between 3.12 and 4.51 eV for MoO_3 system and from 4.06 to 5.33 eV for V_2O_5, depending on the surface oxygen site. The adsorption of second H atom and formation of water species further decreases energy needed to create vacancy. For H_2O removal, desorption energies are close to 1 eV for both V–O and Mo–O systems. Small values for H_2O species formed at the O(3) site in V_2O_5 system, and for O(2) negative value for O(2) type vacancy in MoO_3 system suggest spontaneous generation of point defects at these surface sites. To conclude one has to say that the reduction of energy required forming vacancy follows from the H-induced weakening of the Mo–O and V–O bonds as well as from the exceptional stabilization of free OH and H_2O species as compared to bare O atom. Fig. 4 gives a summary of the energetic data connected with the process of vacancy formation for MoO_3 and V_2O_5 systems together with all discussed schemes leading to the different types of surface vacancies.

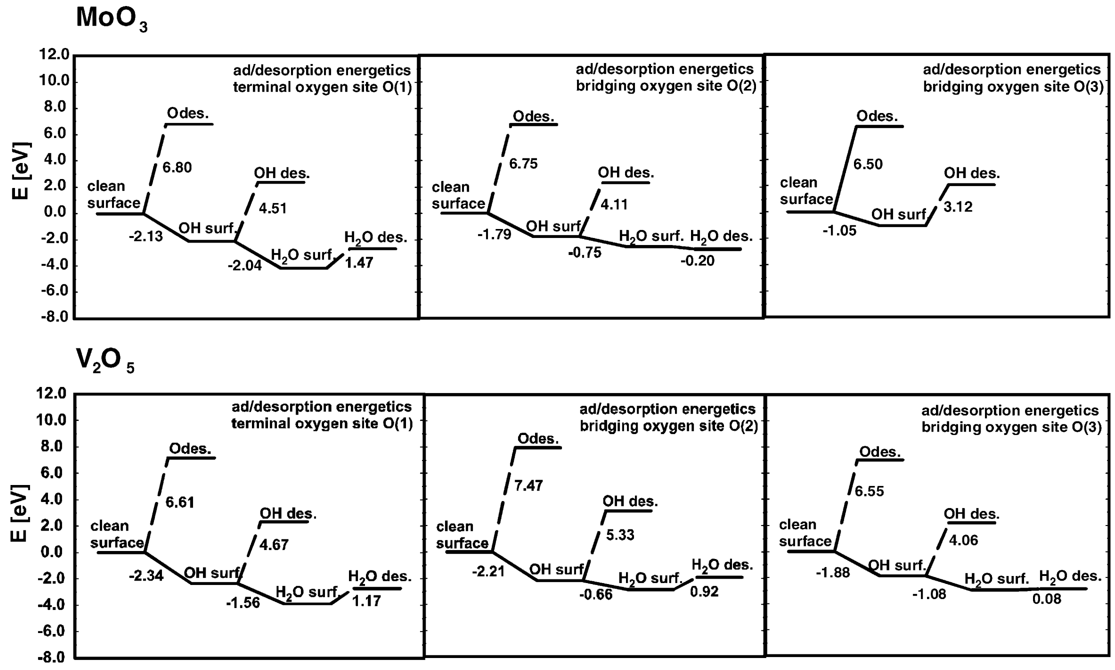

Fig. 4. Energetic scheme of formation of different type of oxygen vacancy as results of removal O, OH, H_2O in the case of MoO_3 and V_2O_5 oxides.

3.5. Relaxation effects of defected surfaces

Formation of oxygen vacancies is accompanied by lowering the coordination numbers of the nearest neighbors. Unbalanced coordination in the vicinity of the point defect is the driving force for structure relaxation of the defected surface. The energetic effect connected with relaxation is different for each type of vacancy and can be described by the relaxation energy calculated as follows:

$$E_{\text{relax}} = E_{\text{D}}^{\text{f}}(\text{O}) - E_{\text{D}}^{\text{r}}(\text{O})$$

where $E_{\text{D}}^{\text{f}}(\text{O})$ refers to the vacancy formation energy calculated for "frozen" cluster (with all atoms kept fixed at their crystallographic positions), whereas $E_{\text{D}}^{\text{r}}(\text{O})$ describes the energy of vacancy formation in a cluster where all atoms (except the terminal H atoms) are allowed to freely rearrange acquiring the lowest cluster energy. Formation of oxygen vacancies at the surfaces leads to the changes in surface geometry that strongly depends on the vacancy type (number of coordination of the missing oxygen atoms) and chemical formula of the system.

From Table 4, which collects the relaxation energies for both MoO_3 and V_2O_5 systems, it is evident that relaxation effect is more pronounced for molybdenum trioxide than for vanadium pentoxide. At (0 1 0)MoO_3 surfaces geometrical changes resulting from the formation of oxygen vacancies are significant [57], especially those connected with the removal of O(1) and O(2) oxygen atoms. In the case of (0 1 0)V_2O_5 surface the rearrangement of bonds following from the vacancy creation is negligible [54] and therefore has a smaller impact on the values of relaxation energies. A source of the different behavior of both systems is their different (bi- and mono-layered) crystallographic structure.

The relaxation effect is always found to be locally confined. As an example, Fig. 5 shows the relaxation effect in closest vicinity of O(2) type vacancy for both systems. White balls denote the positions of atoms in the system without vacancy, whereas the dark balls show the effect of relaxation after removal of O(2) bridging oxygen (system with vacancy).

Detailed analysis of the positions of each atom done for MoO_3 leads to the conclusion that desorption of O(2) bridging oxygen causes the singly coordinated oxygen O(1) to move towards the position of the doubly coordinated. In fact, the same is true other way around i.e. after removal of singly coordinated oxygen bridging oxygen shifts towards vanadyl position. In effect, in both cases major changes in molybdenum coordination close to vacancy site are observed and the same final geometrical structure is obtained i.e. oxygen vacancy that is neither of pure O(1) or O(2) type but something in between. Removal of O(3) oxygen atom leads only to a small rearrangement in cluster geometry, which is reflected by the smallest relaxation energy for this type of vacancy.

Table 4
Energy of relaxation [eV] of defected (0 1 0)V_2O_5 and (0 1 0)MoO_3 surfaces

O(1) vacancy	O(2) vacancy	O(3) vacancy
MoO_3		
1.96	1.92	0.47
V_2O_5		
0.69	0.76	0.52

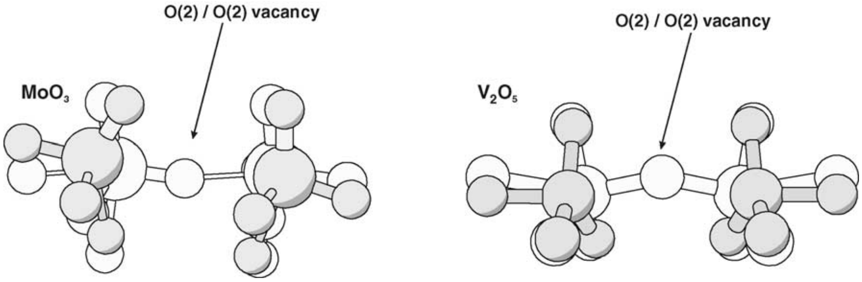

Fig. 5. Relaxed geometry in the closest neighboring of O(2) type vacancy formed at (0 1 0)MoO_3 and (0 1 0)V_2O_5 surfaces.

In the case of V_2O_5 system the relaxation effect is smaller. Relaxation geometry of the closest neighborhood of O(2) type vacancy shown in Fig. 5 leads to the atom displacements of about to 0.6–0.7 Å near the vacancy site (the same effect is observed for O(3) vacancy). After removal of vanadyl oxygen, O(1), only the vanadium atom missing the vanadyl relaxes and moves down into the bulk, which indicates that a single vacancy will not introduce a major restructuring of the surface. Small surface relaxation due to vacancy formation, in V_2O_5 system, decreases the energy of vacancy formation by 0.52–0.76 eV, the effect being the largest for the O(2) site.

3.6. Electronic structure of the defected surfaces

Formation of oxygen point defects leads always to the changes in the electronic structure of transition metal oxides surfaces. Removal of oxygen atom may results in trapping an electron in the formed cavity (effect observed for the ionic system [71,72]) or may lead to the formation of dangling bonds (main effect in the covalent systems [69,70]). The mixed ionic-covalent character of both MoO_3 and V_2O_5 systems and the existence of free d orbitals generate rather complicated nature of oxygen vacancy. In order to elucidate the electronic properties of oxygen vacancies two approaches are applied: without and with oxygen basis in the cavity. The description is done using atomic charges and density of states.

Table 5 collects changes in charges (Mulliken analysis) of metal ions that are close to the vacancy site for Mo–O and V–O systems, obtained without and with the oxygen basis set put in oxygen vacancy. Positive numbers indicate reduction of metal centers whereas negative ones – their oxidation. Reduction of metal ions is connected with formation of oxygen vacancies through the removal of neutral oxygen atoms. After vacancy creation two electrons associated with surface O^{2-} ion remain at the surface and are distributed over the atoms close to the cavity.

Table 5
Changes in populations of metal ions close to vacancy sites as a result of vacancy formation with respect to the clean surface obtained with or without (values in parenthesis) basis set put into the vacancy place

O(1) vacancy	O(2) vacancy	O(3) vacancy
MoO_3		
0.46 (0.41)	0.88 (0.64)	0.48 (0.46)
	0.08 (0.17)	0.46 (0.42)
		0.49 (0.29)
V_2O_5		
0.17 (0.12)	0.31 (0.27)	0.28 (0.27)
	0.31 (0.27)	0.33 (0.24)
		0.28 (0.19)

Positive values indicate the reduction of metal centers.

In all systems changes in populations on metal ions depends on oxygen vacancy type. Results of Mulliken analysis indicate that only metal atoms, which are characterized by incomplete environment, undergo reduction. The compensating charge is uniformly spread over the metal centers in the first coordination shell around the vacancy whereas the charge distribution on the other atoms of the cluster remains nearly the same. Thus, the process of the redistribution of excess electrons has a local character.

In MoO_3 system, the formation of oxygen vacancy leads to the reduction of molybdenum ions by almost 0.4–0.5e per each Mo atom, with the exception of O(2) type vacancy. After removal of O(2), only the molybdenum atom bound to this oxygen by short bond (1.73 Å) is reduced (decrease in positive charge by 0.88); populations on the second Mo atom connected to O via long bond (2.02 Å) changes only slightly (0.08). This is in agreement with the specific character of the O(2) center in MoO_3. As it was mentioned before, doubly coordinated O(2) exhibits many properties of singly coordinated, molybdenyl oxygen. In the presence of oxygen basis placed at the vacancy place, the reduction of molybdenum ions is smaller than in the system without basis, nevertheless it is still pronounced (0.41 for one atom, 0.81 for two atoms and 1.17 for three atoms in case of O(1), O(2) and O(3) vacancy, respectively).

Formation of oxygen vacancy in V_2O_5 oxide results also in the reduction of vanadium atoms, however the values describing the changes in metal population are smaller in comparison to molybdenum trioxide case. The smallest reduction is found for removal of singly coordinated oxygen, O(1) (the positive charge of V atom changes by 0.17 whereas in other cases by 0.3e). Similar as in MoO_3 system, presence of oxygen basis in the vacancy place leads to the smaller reduction (0.12 per one atom, 0.54 per two atoms and 0.70 per three atoms for O(1), O(2) and O(3) vacancy, respectively) in comparison to system without basis set.

Table 6
Accumulation of electrons in the vacancy place

	O(1) vacancy	O(2) vacancy	O(3) vacancy
Mulliken analysis/Löwdin analysis			
MoO_3	0.00e/0.22e	0.00e/0.32e	0.06e/0.43e
V_2O_5	0.00e/0.20e	0.04e/0.29e	0.10e/0.45e

The electrons left behind after the removal of a neutral oxygen atom from the perfect crystal can be delocalized over the ions around the cavity (as shown before), however part of them can be trapped and localized in the center of the vacancy, where the basis set is localized. To study this well-known effect in ionic solids (like MgO [71,72]) Löwdin population analysis is applied, which suit better ionic type interactions than Mulliken one. Table 6 summarizes the values of electron localization in the different vacancies, for both Mulliken and Löwdin approaches for V_2O_5 and MoO_3 oxide.

Results of Mulliken and Löwdin population analyses, which are performed with basis left at the vacancy hole, show that the accumulation of electrons may take place for both metal oxides and is connected rather with vacancy created by desorption of high-coordinated oxygen centers. As expected, Löwdin analysis give more pronounced indication of electron accumulation than Mulliken one; both show the trapping of electrons being the largest in case of vacancy formed by removal of triply coordinated oxygen.

The negative charge (Löwdin analysis) trapped in the O(3) vacancy site (−0.43 for MoO_3 and −0.45 for V_2O_5) is larger than the charge of the respective surface oxygen ion that is missing (−0.31 for MoO_3 and −0.43 for V_2O_5), what means that high coordinated vacancy form a new surface center of higher nucleophillicity than surface oxygen. Taking into account that formation of triply coordinated oxygen vacancy leads to the smallest changes in geometry (see Table 4, energy of relaxation), this type of vacancy may be responsible for formation of color centers at the (0 1 0)V_2O_5 and (1 0 1)MoO_3 surfaces. The accumulation of electrons is smaller in the vacancy, which is made after removal of doubly coordinated oxygen site; at the same time the larger changes in populations of nearby metal ions are observed (see Table 5). The smallest electron density in the vacancy place is found in the case of the vacancy created on the vanadyl or molybdenyl oxygen atom (O(1) type). However, still vacancies are more nucleophilic (0.20e in V_2O_5 and 0.22e in MoO_3) than the singly coordinated oxygen lattice ions (charge on O(1) equals to −0.14 in V_2O_5 and to −0.09 in MoO_3). In all cases not only electrons from the oxygen atoms but also electrons from metal ions coordinated with this oxygen are trapped in the vacancy, which leads to the increase of positive charge on the metal center, and growth of the electrophilic character of the unsaturated metal ions. One should add that in contrast to the large redistribution of charge on metal atoms, close to the

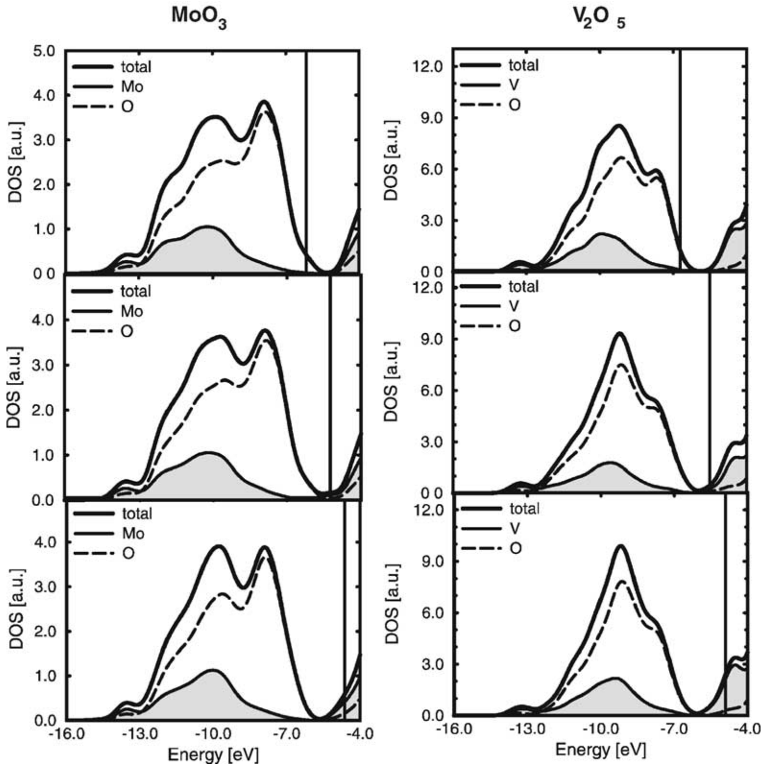

Fig. 6. DOS for $M_{15}O_{56}H_{22}$ cluster described (0 1 0)MoO_3 oxide before and after formation O(3) type vacancy. Total DOS curve (thick solid) with decomposition into molybdenum (thin solid) and oxygen (dashed) contributions. In both the figures a Gaussian broadering of 0.4 eV is applied. The energetic position of the highest occupied cluster orbital E_{HOMO} is marked by a thin vertical line.

vacancy site, oxygen centers near the vacancy show only negligible changes in their charges.

Reduction of metal ions is clearly seen also on projected density of states plots (DOS) see Fig. 6. For both oxides valence region of DOS is characterized by multi-peak structure dominated by oxygen contributions. The lower part of unoccupied band is dominated by metal (V/Mo) contributions that are identified as Mo 4d or V 3d. Formation of oxygen vacancy is associated with only small differences in the valence band region that is characterized by O 2sp. Reduction of metal ions in pure Mo–O and V–O systems, corresponds to adding electrons to the low-lying empty Mo 4d/V 3d levels, which contribute to the bottom of the conduction band. In effect, by adding point defects (first and second vacancy) the HOMO level is shifted towards metal d orbitals.

Thus, formation of oxygen point defects (mono- or di-vacancy) creates new reactive energy levels that are illustrated on molecular orbital diagrams given in Fig. 7. For both oxides formation of mono-vacancy by removal of O(2) or O(1) atoms creates a localized doubly occupied state that lies near the conduction band whereas in the case of O(3) vacancy that state is placed in the middle between valence and conduction bands. Formation of di-vacancy results in additional occupied state, which is located between the valence and conduction bands. This leads to the decrease of HOMO–LUMO energy gap and can be seen as a first step towards transformation from isolator into metal. The additional level between conduction and valence band may become also responsible for changes in the reactivity of the defected surface.

3.7. Reactivity of vacancies

All created surface vacancies may become re-oxidized either through exchange with gaseous oxygen or via diffusion of bulk oxygen atoms. More detailed information on this reaction proceeding due to O_2 adsorption is given in [73,74], here only the main conclusions are given for completeness of the description of surface transformation.

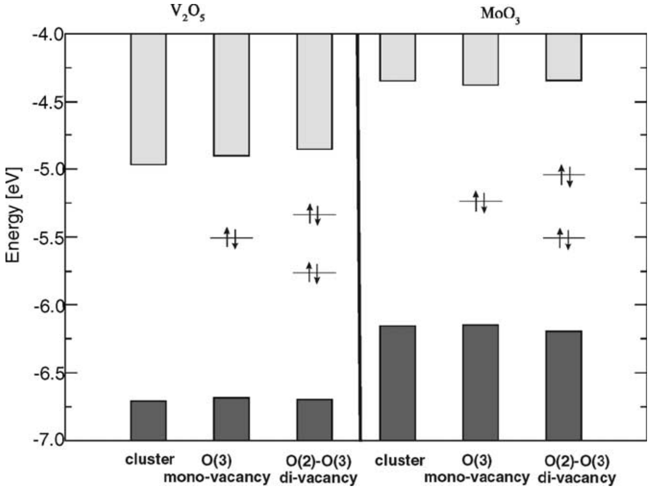

Fig. 7. Molecular energy diagram showing the changes in HOMO and LUMO levels upon O(3) mono-vacancy and di-vacancy formation in V_2O_5 and MoO_3 oxide with comparison with non-defected surfaces.

Molecular oxygen becomes adsorbed (exothermic process) at any surface vacancy in geometries given in Fig. 8. The ordering of adsorption energies (see Table 7) goes parallel with the energies required to form vacancy i.e. the most difficult vacancy to create – is the first to be filled. Upon stabilization at surface the molecular oxygen undergoes activation (weakened and stretched O–O bond). Thus, adsorbed molecular oxygen can replace the surface oxygen occupying a specific lattice site, which means that the oxide surface is able to incorporate larger amount of oxygen species than follows from its stoichiometry.

In order to restore the initial state one oxygen atom has to be removed after the O_2 molecule is adsorbed at the vacancy. The energies corresponding to the removal of oxygen, (E_B(O)), which are equal (with opposite sign) to the energies

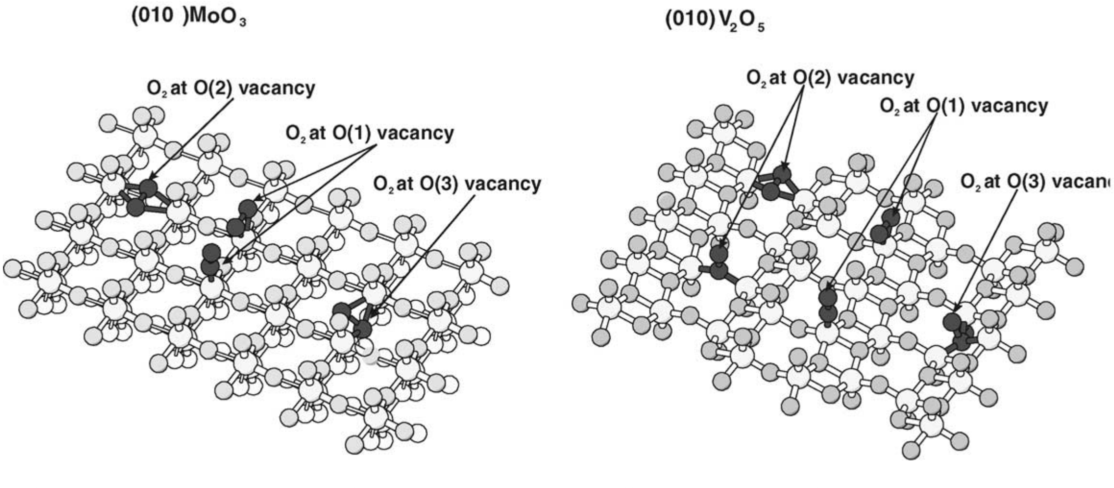

Fig. 8. Sketch of computed equilibrium geometries of an adsorbed O_2 molecule at different vacancy sites of the MoO_3(0 1 0) and V_2O_5(0 1 0) surfaces. The results are obtained by optimizing the O_2 position and geometry in the $Mo_{15}O_{55}H_{22}$ and $V_{10}O_{30}H_{12}$ vacancy cluster models. Shaded balls show the O_2 adsorbate species while the surface lattice is sketched by lighter balls.

Table 7
Energies of vacancy formation E_D, molecular oxygen adsorption at a vacancy $E_B(O_2)$, and atomic oxygen adsorption at the surface $E_B(O)$ for surface sites O(1), O(2), O(3) at the (0 1 0)MoO_3 and (0 1 0)V_2O_5 surfaces using $Mo_{15}O_{56}H_{22}$ and $V_{10}O_{31}H_{12}$ clusters, respectively

Geometry	Parallel/perpendicular O(1) vacancy	Parallel/perpendicular O(2) vacancy	Parallel O(3) vacancy
MoO_3			
$E_B(O_2)$	−2.98/−2.39	−1.11/–	−0.08
$E_B(O)$	−1.77/−1.19	−0.02/–	0.82
V_2O_5			
$E_B(O_2)$	−2.53/−2.16	−3.27/−2.76	−1.03
$E_B(O)$	−1.50/−1.13	−1.38/−0.87	0.05

All energies are given in eV.

of adsorption of atomic oxygen, are listed also in Table 7. For both oxides, the removal of O atom from O_2 molecule adsorbed at the O(3) vacancy is spontaneous. Small, negative values of $E_B(O)$ for all other cases indicate the presence of easily released active oxygen atom.

4. Conclusions

The performed calculations show the possibility of different active centers that may exist at the oxide surface: surface oxygen and metal sites, local vacancies, adsorbed OH, H_2O and O_2 species. Structurally non-equivalent surface oxygen sites are characterized by different electronic states and, as a result, exhibit different catalytic properties. Lattice oxygen atoms are strongly bound to the surface therefore formation of oxygen vacancies is a highly endothermic process. A prior H adsorption, which results in formation of hydrogen containing surface species (hydroxyl and water) decreases energy required for vacancy creation. Local point defects formed at structurally different places (different number of bonds to be broken, different arrangement) are characterized by various electronic states (different chemical reactivity) and exhibit stronger nucleophilic character than the respective surface oxygen. The preexisting vacancy influences the formation of the second vacancy. Vacancy may aggregate (due to the electrostatic type interaction) giving a first step towards a more pronounced defect. Presence of oxygen vacancies changes the electronic structure of the surfaces, in particular electronic state of metal atoms localized nearby. All surface vacancies may become re-oxidized via gaseous oxygen or through oxygen diffusion from the bulk. Adsorption of O_2 gaseous molecule is an exothermic process and leads to molecular, weakly bonded and very active oxygen species.

Acknowledgements

Authors acknowledge partial financial support from the State Committee for Scientific Research of Poland through a Grant 7 T09A 11921.

References

[1] H.K. Kung, in: B. Delmon, J.T. Yates (Eds.), Transition Metal Oxides: Surface Chemistry and Catalysis, Studies in Surface Science and Catalysis, vol. 45, Elsevier, Amsterdam, 1989.
[2] C.N.R. Rao, B. Raveau, Transition Metal Oxides, VCH Publishers Inc., UK, 1995.
[3] G. Ertl, H. Knozinger, J. Weitkamp (Eds.), Handbook of Heterogeneous Catalysis, Wiley/VCH, Weinheim, 1997, p. 2253, and references therein.
[4] V.E. Henrich, P.A. Cox, The Surface Science of Metal Oxides, University Press, Cambridge, 1994.
[5] E.M. Gaigneaux, H.M. Abdel Dayem, E. Goddard, P. Ruiz, Appl. Catal. A: Gen. 202 (2000) 265.
[6] P.J. Gellings, H.J.M. Bouwmeester, Catal. Today 58 (2000) 1.
[7] S. Surnev, M.G. Ramsey, F.P. Netzer, Prog. Surf. Sci. 73 (2003) 117.
[8] B. Grzybowska-Świerkosz, F. Trifiro, Appl. Catal. A 1/2 (1997) 157, and references therein.
[9] G.C. Bond, S.F. Tahir, Appl. Catal. 71 (1991) 1.
[10] B. Grzybowska-Świerkosz, Topics Catal. 21 (2002) 35, and references therein.
[11] G. Centi, F. Cavani, F. Trifiro, Selective Oxidation by Heterogeneous Catalysis, Kluwer Academic Publishers, 2001.
[12] F. Cavani, F. Trifiro, Stud. Surf. Sci. Catal. 110 (1997) 19.
[13] F. Cavani, F. Trifiro, Catal. Today 36 (1997) 431.
[14] E.R. Braithwaite, J. Haber (Eds.), Molybdenum: An Outline of its Chemistry and Uses, Studies in Inorganic Chemistry, vol. 19, Elsevier, Amsterdam, 1994.
[15] G. Mestl, T.K.K. Srinivasan, Catal. Rev. -Sci. Eng. 40 (4) (1998) 451.
[16] R. Pearce, W.R. Patterson (Eds.), Catalysis and Chemical Processes, Wiley/Halsted, New York, 1981.
[17] A.M. Chippindale, A.K. Cheetham, in: E.R. Braithwaite, J. Haber (Eds.), The Oxide Chemistry of Molybdenum, Studies in Inorganic Chemistry, vol. 19, Elsevier, Amsterdam, 1994.
[18] J. Haber, E. Lalik, Catal. Today 33 (1997) 119.
[19] A. Bielanski, J. Haber, Oxygen in Catalysis, Marcel Dekker, New York, 1991.
[20] M. Che, A.J. Tench, Adv. Catal. 31 (1982) 78.
[21] M. Che, A.J. Tench, Adv. Catal. 32 (1983) 1.
[22] J.S. Anderson, R.J.D. Tilley, in: M.W. Roberts, J.M. Thomas (Eds.), Surface and Defect Properties of Solids, vol. 3, The Chemical Society, London, 1974, p. 1.
[23] G. Mestl, Ch. Linsmeier, R. Gottschall, M. Dieterle, J. Find, D. Herein, J. Jäger, Y. Uchida, R. Schlögl, J. Mol. Catal. A 162 (2000) 463.
[24] P.L. Gai-Boyes, Catal. Rev. -Sci. Eng. 34 (1992) 1.
[25] P. Ruiz, B. Delmon (Eds.), New Developments in Selective Oxidation by Heterogeneous Catalysis, Studies in Surface Science and Catalysis, vol. 72, Elsevier Science Publishers, 1992.
[26] N.N. Greenwood, Ionic Crystal, Lattice Defects and Nonstoichiometry, Butterworths, London, 1968.
[27] C.A. Catlow, in: O.T. Sorensen (Ed.), Nonstoichiometric Oxides, Academic Press, 1981.
[28] K. Bruckman, R. Grabowski, J. Haber, A. Mazurkiewicz, J. Sloczynski, T. Wiltowski, J. Catal. 104 (1987) 71–79.
[29] P. Mars, D.W. van Krevelen, Chem. Eng. Sci. 3 (1954) 41 (special supplement).
[30] A. Magneli, Nature 115 (1950) 356.
[31] A. Magneli, Ark. Kemi 1 (1950) 513.
[32] J. Haber, M. Witko, R. Tokarz, Appl. Catal. A 1/2 (1997) 3, and references therein.
[33] J. Haber, E. Lalik, Catal. Today 33 (1997) 119.
[34] H. Werner, O. Timpe, D. Herein, Y. Uchida, N. Pfänder, U. Wild, R. Schlögl, H. Hibst, Catal. Lett. 44 (1997) 153.
[35] E. Serwicka, J. Solid State Chem. 51 (1984) 300.
[36] E. Serwicka, Crit. Rev. Surf. Sci. 1 (1) (1990) 27.
[37] M. Łabanowska, Phys. Chem. Chem. Phys. 1 (1999) 5385.

[38] M. Łabanowska, Chem. Phys. Chem. 2 (2001) 712.

[39] G. Mestl, N.F.D. Verbruggen, H. Knözinger, Langmuir 11 (1995) 3035.

[40] T. Ressler, O. Timpe, T. Neisius, J. Find, G. Mestl, M. Dieterle, R. Schlögl, J. Catal. 191 (2000) 75.

[41] T. Ono, H. Numata, N. Ogata, J. Mol. Catal. A: Chem. 105 (1996) 31.

[42] X. Ni, G. Sun, M. Ceolin, M.A. Taylor, W. Tröger, T. Butz, Chem. Phys. 223 (1997) 109.

[43] E.N. Voskresenskaya, V.G. Rogguleva, A.G. Anshits, Catal. Rev. -Sci. Eng. 37 (1) (1995) 101.

[44] R. Schaub, P. Thostrup, N. Lopez, E. Lægsgaard, I. Stensgaard, J.K. Nørskov, F. Besenbacher, Phys. Rev. Lett. 87 (26) (2001) 266104.

[45] M. Chen, C.M. Friend, E. Kaxiras, J. Am. Chem. Soc. 123 (2001) 2224.

[46] C. Nuguera, in: D.P. Woodruff (Ed.), Oxide Surfaces, Elsevier Science, 2001, p. 35.

[47] C.A. Catlow, in: K. Wright, R. Catlow (Eds.), Microscopic Properties in Minerals, Kluwer Academic Publishers, The Netherlands, 1999.

[48] O.T. Sorensen (Ed.), Nonstoichiometric Oxides, Academic Press, 1981.

[49] A. Kämper, I. Hahndorf, M. Bearns, Top. Catal. 11/12 (2000) 77.

[50] M.J. Puska, S. Pöykkö, M.M. Pesola, R.M. Nieminen, Phys. Rev. B 58 (1998) 1318.

[51] K. Hermann, M. Witko, R. Druzinic, Faraday Discuss. 114 (1999) 53.

[52] K. Hermann, M. Witko, R. Druzinic, R. Tokarz, Top. Catal. 11/12 (2000) 67.

[53] K. Hermann, M. Witko, in: D.P. Woodruff (Ed.), Oxide Surfaces, Elsevier, Amsterdam, 2001, p. 136.

[54] K. Hermann, M. Witko, R. Druzinic, R. Tokarz, Appl. Phys. A 72 (2001) 429.

[55] J. Haber, M. Witko, J. Catal. 216 (2003) 416.

[56] R. Tokarz-Sobieraj, K. Hermann, M. Witko, A. Blume, G. Mestl, R. Schlögl, Surf. Sci. 489 (2001) 107.

[57] R. Tokarz-Sobieraj, K. Hermann, M. Witko, manuscript in preparation.

[58] M. Witko, R. Tokarz-Sobieraj, R. Grybos, in: N. Russo, D.R. Salahub, M. Witko (Eds.), NATO Science Series, Metal–Ligand Interactions, Kluwer Academic Publishers 116 (2003) 301.

[59] R.W.G. Wyckoff, Crystal Structures, Interscience/Wiley, New York/London, 1965.

[60] J.K. Labanowski, J.W. Andzelm (Eds.), Density Functional Methods in Chemistry, Springer-Verlag, New York, 1991.

[61] N. Godbout, D.R. Salahub, J.W. Andzelm, E. Wimmer, Can. J. Phys. 70 (1992) 560.

[62] The program package StoBe is a modified version of the DFT-LCGTO program package DeMon, originally developed by A. St.-Amant and D. Salahub (University of Montreal), with extensions by L.G.M. Petterson and K. Hermann.

[63] J.P. Perdew, K. Burke, M. Ernzerhof, Phys. Rev. Lett. 77 (1996) 3865.

[64] B. Hammer, L.B. Hansen, J.K. Norskov, Phys. Rev. B 59 (1999) 7413.

[65] J. Andzelm, E. Radzio, D.R. Salahub, J. Chem. Phys. 83 (1985) 4573.

[66] R.S. Mulliken, J. Chem. Phys. 23 (1955) 1833, 1841, 2388, 2343.

[67] I. Mayer, Chem. Phys. Lett. 97 (1983) 270.

[68] I. Mayer, J. Mol. Struct. (Theochem) 149 (1983) 270.

[69] G. Pacchioni, Solid State Sci. 2 (2000) 161.

[70] D. Erbetta, D. Ricci, G. Paccioni, J. Chem. Phys. 113 (2000) 10744.

[71] A.M. Ferrari, G. Paccioni, J. Phys. Chem. 99 (1999) 17010.

[72] J. Chen, L. Lin, F. Jing, Nucl. Instr. Meth. Phys. Res. B 187 (2002) 354.

[73] R. Tokarz-Sobieraj, R. Grybos, M. Witko, Ann. Pol. Chem. Soc. 2 (III) (2003) 936.

[74] R. Tokarz-Sobieraj, R. Grybos, M. Witko, K. Hermann, Collect. Czech. Chem. Commun. 69 (2004) 121.